Available online at www.sciencedirect.com
ScienceDirect
Journal of Power Sources 160 (2006) 1183–1194
JOURNAL OF POWER SOURCES
www.elsevier.com/locate/jpowsour

Development of planar air breathing direct methanol fuel cell stacks

Zhen Guo, Amir Faghri *

Department of Mechanical Engineering, University of Connecticut, Storrs, CT 06269, United States

Received 6 February 2006; received in revised form 10 March 2006; accepted 10 March 2006
Available online 24 April 2006

Abstract

In this paper, design criteria and development techniques for planar air breathing direct methanol fuel cell stacks are described in detail. The fuel cell design in this study incorporates a window-frame structure that provides a large open area for more efficient mass transfer and is modular, making it possible to fabricate components separately. The membrane electrode assembly and gas diffusion layers are laminated together to reduce contact resistance, which eliminates the need for heavy hardware. The composite current collector is low cost, has high electrical conductivity and corrosion resistance. In the interest of quick and cost-efficient prototyping, the fabrication techniques were first developed on a single cell with an active area of 1.0 cm^2. Larger single cells with active areas of 4.5 and 9.0 cm^2 were fabricated using techniques based on those developed for the smaller single cell. Two four-cell stacks, one with a total active area of 18.0 cm^2 and the other with 36.0 cm^2, were fabricated by inter-connecting four identical cells in series. These four-cell stacks are suitable for portable passive power source applications. The performance analysis of single cells as well as stacks is presented. Peak power outputs of 519.0 and 870.0 mW were achieved in the stacks with active areas of 18.0 and 36.0 cm^2, respectively. The effects of methanol concentration and fuel cell self-heating on the fuel cell performance are emphasized.

Keywords: Direct methanol fuel cell; Fuel cell stack; Air breathing; Planar

1. Introduction

Portable power is becoming important for many electronic devices, such as notebook computers, personal digital assistants (PDAs), music systems and cellular telephones. Currently, these devices are powered by primary and secondary batteries. While the power source is often the largest component of the device and, in fact, is the limiting factor in efforts toward miniaturization, the runtime and functionality of the devices remain limited by the quantity of energy that can be stored and carried within them [1–3]. Thus, advances in the development of portable fuel cells will have a great impact on the use and development of modern electronic devices. Portable power devices are also gaining importance in security applications. Batteries limit equipment functionality, and thus the mission length allotted soldiers using the equipment, to approximately several hours. Miniature fuel cells, which promise higher energy densities and instant refueling, present opportunities for use as supplements to, or substitutes for, batteries that may extend mission time, perhaps to several days [4].

Unlike primary and secondary batteries, where the reactants and products are contained within the battery, fuel cells employ reactants that are continuously supplied to the cell; byproducts also are continuously removed. Although other oxidants are theoretically possible, oxygen is the standard because it is readily available in the atmosphere. Typical fuels used in a fuel cell are hydrogen or a liquid organic fuel (i.e., methanol, formic acid). Liquid fuels, which offer ready availability, easy storage and handling, and high energy density, are well-suited for portable fuel cells. However, with the exception of methanol, liquid fuels simply do not react at a sufficient rate to warrant consideration [5]. As will be discussed shortly, methanol must be mixed with water before it is introduced into the anode of a proton exchange membrane fuel cell. Such fuel cells are called “direct methanol” fuel cells. This fuel cell is in contrast to a fuel cell that uses hydrogen produced from methanol in a reformer.

In practice, fuel cells do not operate as single units; rather, they are connected in a series to additively combine the individual cell potentials and achieve a greater, and more useful, potential. A collection of single cells in series is known as a

* Corresponding author. Tel.: +1 860 486 2221; fax: +1 860 486 0318.
E-mail address: faghri@engr.uconn.edu (A. Faghri).

0378-7753/$ – see front matter © 2006 Elsevier B.V. All rights reserved.
doi:10.1016/j.jpowsour.2006.03.045

"stack". For conventional actively-driven fuel cells, the most popular means of interconnection is to use a "bipolar plate". This plate makes a connection between one cathode and the anode of the next cell, while the bipolar plate serves as a means of feeding oxygen to the cathode and fuel to the anode. The fuel cell stack consists of a repeated, interleaved structure of membrane electrode assemblies (MEAs), gas diffusion layers (GDLs) and bipolar plates. All these components are clamped together with significant force to reduce electrical contact resistance. The fuel and oxidant are provided with manifolds to the correct electrodes, and cooling is provided either by the reactants or by a cooling medium. Usually, this type of fuel cell works with forced airflow on the cathode side and forced fuel flow on the anode side, requiring various auxiliary components and a rather complicated control system [6]. Such a fuel cell does not fit the requirements for low-power-battery replacement applications.

For such applications, the key challenges are to provide acceptable power output and high-energy efficiency under conditions convenient to the user. The typical desired operating conditions include, for example, an operating temperature near room temperature, no forced airflow, and no recirculation fuel pump. It is well known that a forced air design with an external blower is unattractive for use in small fuel cell systems, as the parasitic power losses from the blower are estimated at 20–25% of the total power output. The passive air breathing operation mode is used in most small fuel cell designs [7–9].

The unique requirements of air breathing small fuel cells have led to several alternative designs. U.S. Patent No. 6,596,422 provided an air breathing direct methanol fuel cell structure [10]. In this design, perforated metal sheets replaced flow channel plates for current-collecting purposes, and holes were made in positive and negative end plates to permit natural diffusion of air to the cathode and fuel to the anode. Similar positive and negative end plates are also used in U.S. Patent No. 6,689,502 [11]. To supply fuel and oxygen continuously to the cell, the fuel and oxygen must penetrate through the holes in the negative and positive end plates, respectively. The byproduct, such as CO_2 at the anode in direct methanol fuel cells (DMFCs), exits the cell through these holes at the negative end plates. The open area ratio, defined as the total area of holes to total area of the end plate, is about 40–60% for these end plates. As a result, the area available for the diffusion of fluids (fuel, oxygen and byproducts) is reduced accordingly and the diffusion path length is increased due to the thickness of the end plate. Both of these effects introduce the mass transfer limitation problem and lower the cell's power density ($mW\,cm^{-2}$).

Single cells can be electrically connected to form a fuel cell stack, such as a planar fuel cell stack. U.S. Patent No. 6,689,502 disclosed a planar fuel cell stack that used common current collectors to connect the anodes and cathodes of the adjacent single cells [11]. The drawback of these designs is that the stack and associated hardware are too heavy for many small applications, such as portable devices and personal use. All of the components are clamped together with significant force (as is done in conventional actively-driven fuel cells) to reduce electrical contact resistance; the end plates used to sustain this force are usually very heavy.

The fuel cell design in this study fulfills the requirements for small applications and portable devices. The cell is passive and air breathing and operates at convenient conditions to the user, which eliminates the need for ancillary equipment. The MEA and GDL are laminated together to reduce contact resistance. The design is also modular in nature, which allows the components to be fabricated separately and configured to meet specific power requirements.

2. Development techniques highlights

Fig. 1 shows the schematic diagram of a single cell structure proposed and evaluated in the study. The cell consists of a catalyst-coated membrane, anode-backing layer, cathode-backing layer, metal current collectors and fixture frames. The catalyst-coated membrane was created by first coating catalyst materials on Teflon® decals by using the screen-printing technique, and then transferred to Nafion® 117 via hot-press. The metal loading level is $6.5\,mg\,Pt\,cm^{-2}$ for the cathode and $7.0\,mg\,Pt{:}Ru\,(1{:}1)\,cm^{-2}$ for the anode. The gas diffusion media were carbon-cloth-based substrates (E-Tek V2.02 at the anode and V2.1-11 at the cathode). The current collector may be a sheet of either expanded metal mesh or wire mesh, though an expanded metal mesh is preferable. Ideally, the expanded metal mesh or other electrically conductive material will have a large proportion of open area to minimally affect mass transport. The fixture frame structure design facilitates the fluid flow and minimizes the weight of the cell. Table 1 summarizes the important technical parameters related to development of planar air breathing direct methanol fuel cell stacks. A few of these development techniques are highlighted in this section.

2.1. Design of the fixture frame

Five different frame structures, as shown in Fig. 2, were evaluated in experiments. The frame shown in Fig. 2A, the simplest structure, was used to fabricate single cells with an active area of $1.0\,cm^2$. The fundamental development techniques were first developed on this small cell to facilitate speed and cost-efficient prototyping. The frame shown in Fig. 2B and C were

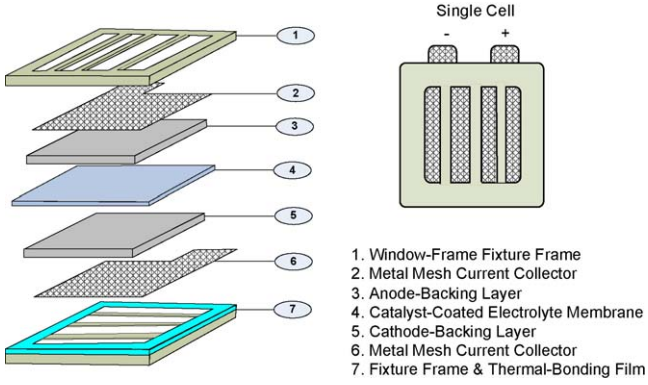

Fig. 1. A single cell with a window-type fixture frame structure suitable for air breathing and fuel diffusion.

Table 1
Selected important parameters in developing the planar air breathing DMFC stacks

Fixture frame	Expanded metal mesh	Anode-backing layer	Anode catalyst layer	PEM	Cathode catalyst layer	Cathode-backing layer	Expanded metal mesh	Thermal-bonding film
(a) Active area of each cell (e.g., 1.0, 4.5 and 9.0 cm^2)	(a) Material (e.g., stainless steel, titanium and copper)	(a) Composition (e.g., carbon black, carbon fiber and binder polymer)	(a) Catalyst selection (e.g., PtRu)	(a) PEM selection (e.g., Nafion®)	(a) Catalyst selection (e.g., Pt)	(a) Thickness (e.g., 0.36 mm)	(a) Hydrophobic treatment of mesh surface	(a). Bond/cure time (e.g., 2–5 s)
(b) Number of cells in one frame (e.g., 1–4)	(b) Platinum-plated or not	(b) Treatment (e.g., temperature and protective gas)	(b) Catalyst loading (e.g., 7.5 mg cm^{-2})	(b) Thickness of the PEM	(b) Catalyst loading (e.g., 6.5 mg cm^{-2})	(b) PTFE loading	(b) Contact resistance with CBL	(b) Bond line temperature (e.g., 135 °C)
(c) Cell active area shape (e.g., square and circle)	(c) Open area of the mesh (e.g., 66%)	(c) Porous structure (e.g., porosity and average pore size)	(c) Nafion® loading (e.g., 2.5 mg cm^{-2})	(c) Methanol crossover	(c) Nafion® loading (e.g., 2.5 mg cm^2)	(c) Electrical resistance of cathode-backing layer (CBL)	(c) Expanded metal patterns	(c) Base resin
(d) Stiffness of frames (e.g., flexible and foldable)	(d) Stiffness of the mesh	(d) Hydrophilic treatment	(d) Porous structure characteristics	(d) Proton conductivity	(d) Porous structure characteristics (e.g., pore size distributions, contact angle and total pore surface area)	(d) Water contact angle in different size pores		(d) Overlap shear strength
(e) Thickness of the frame (e.g., 1.0 mm)	(e) Thickness of the mesh (e.g., 0.16 and 0.54 mm)		(e) Contact resistance with PEM and anode-backing layer	(e) Water management		(e) Capillary pressure at different amounts of the liquid in the CBL		(e) Standard thickness
(f) Reinforced fiberglass frame	(f) Contact resistance with anode-backing layer		(f) Durability in long-term running	(f) Durability in long-term running		(f) Permeability		

used to make larger single cells with an active area of 4.5 and 9.0 cm^2, respectively. The fabrication techniques developed on the smaller single cells were utilized in this scale-up process. Compressive force is needed to hold the electrode backing layers and the catalyst-coated membrane closely together to reduce resistance to ionic and/or electrical flow between the elements. For the small single cells with an active area of 1.0 cm^2, the frame shown in Fig. 2A was used. The frame and the expanded metal mesh provide sufficient compressive force for single cells with a relatively small active area. Ribs were made in the frames, shown in Fig. 2B and C, to provide a even distribution of compressive force for a single cell with a larger active area. The frames shown in Fig. 2D and E were used in developing the DMFC stack with four identical single cells with the frame structures shown in Fig. 2B and C, respectively.

When two frames are clamped together, there are two possible ways to arrange them, as shown in Fig. 3. Two frames are arranged parallel along the ribs in Fig. 3A, and perpendicularly along the ribs in Fig. 3B. The cells that used the perpendicular alignment produced better performance caused by a more even distribution of compressive force over the active area of the fuel cell, which reduces the internal contact resistance.

2.2. Hydrophilic treatment of anode-backing layer

The anode-backing layer is located between the current collector and catalyst layer on the anode side of a fuel cell. This layer is formed from a porous material, which must have high electrical conductivity, high gas permeability, high surface area and good water management characteristics [12]. The anode-backing layer of a DMFC differs from that of hydrogen PEMFCs in that it must be hydrophilic to facilitate the mass transfer of the dilute methanol solution to the anode. Most commercially available GDL products are hydrophobic, necessitating hydrophilic treatment to improve the anode-backing layer's wettability and capability for transferring the dilute methanol solution. One approach for rendering the anode-backing layer more hydrophilic is to partially fill the pores of the carbon porous medium with certain metal oxide compounds. Appropriate metal oxide or hydroxide compounds include tin oxide (SnO_2), aluminum oxide (Al_2O_3), niobium oxide (Nb_2O_5), tantalum oxide (Ta_2O_5), titanium oxide (TiO_2), and ruthenium oxide (RuO_2). Bett et al. [13] provided a method to introduce suitable metal oxides into the carbon porous media, described below:

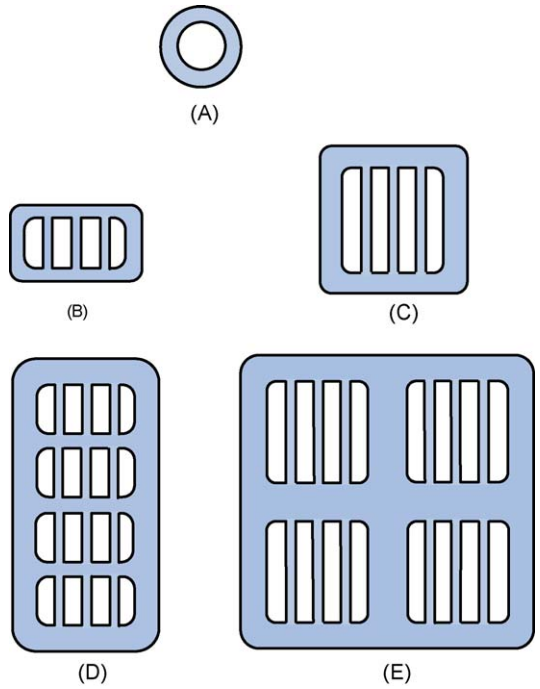

Fig. 2. Five different fixture frames used in the experiments. (A) A single cell with an active area of 1.0 cm^2; (B) a single cell with an active area of 4.5 cm^2; (C) a single cell with an active area of 9.0 cm^2; (D) a four-cell stack with a total active area of 18.0 cm^2; (E) a four-cell stack with a total active area of 36.0 cm^2.

(1) Dissolve tin tetrachloride pentahydrate ($SnCl_4 \cdot 5H_2O$) in water to give a tin tetrachloride concentration of 1.7 mol l^{-1}.
(2) Pour this solution into a vial of sufficient depth to amply submerge carbon fiber media placed therein.
(3) Place the vial in an ultrasonic bath and apply ultrasonic treatment for 10 min.
(4) Remove the carbon fiber medium from the tin tetrachloride solution and put it into an aqueous ammonia solution sufficiently concentrated to achieve a pH of 9.

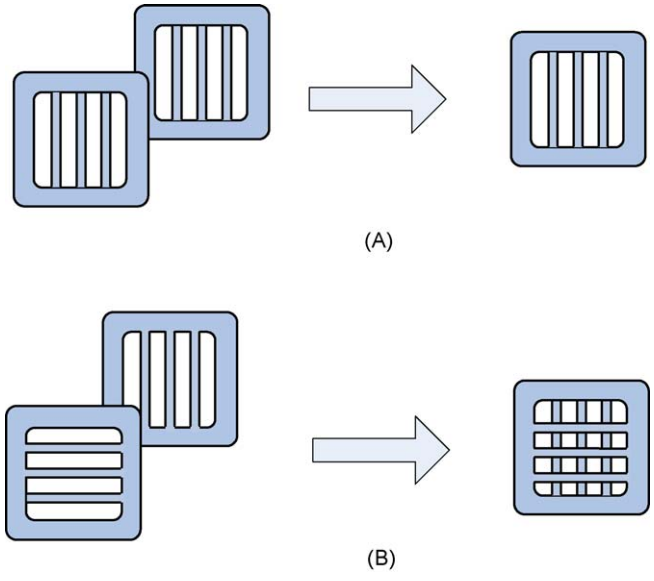

Fig. 3. The relative orientations of two fixture frames in fuel cells: (A) parallel along the ribs; (B) perpendicular along the ribs.

(5) Over a period of 6 h, the ammonia is neutralized by chloride ions released by hydrolysis of the tin chloride in the carbon fiber paper, while the pH of the bulk of the solution is maintained in the range of approximately 5–9 by timely addition of fresh ammonia. In this way the tin chloride in the pores of the carbon fiber paper will be converted to an insoluble tin hydroxide.
(6) After the 6-h immersion, remove the carbon fiber paper from the ammonia solution and calcine in air at a temperature of 400 °C for 1 h.
(7) Repeat steps 1–6 several times to improve the carbon cloth medium's wettability.

The chemical reactions occurring in these processes can be summarized as follows:

$$SnCl_4 + 4NH_4OH \rightarrow Sn(OH)_4\downarrow + 4NH_4Cl \text{ (in ammonia solution)},$$

$$Sn(OH)_4 \rightarrow SnO_2 + 2H_2O \text{ (at 400 °C in oven)}$$

The advantages of this treatment method are two-fold:

(1) *Stability*: Stannic hydroxide has solubility in water of pH 7 below about 10^{-8} mol l^{-1}. Tin oxide (SnO_2) also has a very low solubility in water. Tin oxide will therefore be suitable for hydrophilic treatment of a fine-pore carbon medium.
(2) *Durability*: Although the plain carbon fiber medium can be wetted by water after ultrasonic cleaning, the treated porous carbon medium usually loses its hydrophilic property if exposed to air for several days. After the pores in the anode-backing layers are partially filled with tin oxide, the wettability and water absorption capacity of the carbon body increases. This treatment effect is permanent.

Another hydrophilic treatment method used in our study was first disclosed in U.S Patent No. 6,733,841 [14]. The advantages of this method are simplicity and speed; typical processing time is 15 min.

This method for hydrophilic treatment of an anode-backing layer comprises the following steps:

(1) Immerse the carbon porous medium in an aqueous dispersion of one or more metal oxides, comprising: (i) 1–15% by weight metal oxide; (ii) 0.01–5% by weight surfactant.
(2) Heat the carbon porous medium sufficiently to substantially remove all of the dispersant.

A Nyacol® SN15ES SnO_2 dispersion (Nyacol Nano Technologies, Inc., Ashland, MA) was used for all SnO_2 dispersions. The dispersion contains 15 wt.% SnO_2 as received. SnO_2 particle size is 10–15 nm. Lower SnO_2 content dispersions were made by the addition of deionized water. After dilution, a trace amount of non-ionic surfactant Triton® X100 was added to the SnO_2 dispersion.

2.3. Selection of current collectors

The current collectors have several functions in a passive DMFC stack. First, they must be electrically conductive to reduce the resistance in a cell and connect cells in series. Second, they must be permeable to liquids and gases in order to provide the liquid and gas diffusion paths to cells. Third, they must provide structural support for the MEA, so they must be strong as well as lightweight. In addition, the current collectors must be corrosion-resistant in the fuel cell environment, and made of inexpensive material.

Some of the above requirements may contradict each other; therefore, selection of the current collectors involves an optimization process. The ideal material may not be the best in any one of the property categories but must be the one that best satisfies the optimization criteria (typically determined by the best performance of the fuel cell and availability).

The current collector may be fabricated from a sheet of expanded metal mesh, metal wire mesh, perforated metal, or other electrically conductive sheet with a large portion of open area. A sheet of expanded metal mesh is preferable in the present application. Expanded metal mesh sheets are manufactured from a variety of metals, including titanium, nickel, copper, stainless steel, aluminum, and niobium. They are available from a variety of manufacturers and contain open areas ranging from 10 to 70% of gross space. Compared to expanded metal, perforated metal sheets generally are stronger and more conductive, but they usually have a smaller open fraction (<40%). Woven meshes have more open area (up to 80%) for superior gas/liquid transfer, however, they generally have a higher electrical resistance due to their large number of wire-to-wire contacts.

Since the current collector is quite close to the membrane, it is imperative that the metal does not corrode. Corrosion not only increases the contact resistance between the active portion of the electrode and the current collector, it also will introduce mobile metal ions, which may come into contact with the membrane and replace protons. Replacing even a small fraction of the protons in the membrane with far less-mobile metal ions will lead to a significant drop in membrane conductivity. Both factors can significantly increase the total internal resistance of fuel cells. In practice, a layer of a more precious metal, such as platinum or gold, is plated to a piece of lightweight material to protect it from corrosion and to improve electrical contacts.

Platinum is desirable for use on the surface as a primary current collector coating material due to its excellent corrosion resistance under DMFC working conditions and its ability to pass current without forming an insulating film. The coating layer should be as thin as possible because platinum is an expensive metal. A substrate material also may be used to further reduce reliance on platinum while maintaining the coating layer's structural integrity.

It is important that the substrate is able to form an insulating film under fuel cell working conditions, such that a dimensionally stable current collector with good conductivity is obtained, and at relatively low cost. It is necessary in most cases to use a combination of materials, because no individual material fully meets all of these criteria.

Both niobium and titanium have the ability to form insulating oxide films under fuel cell conditions, and both possess unique advantages and disadvantages as a substrate for platinum. The major advantage of titanium is its low cost, particularly in conjunction with its lower density. A major disadvantage of titanium is its poor electrical conductivity (23.81 1 $m\Omega\,cm^{-1}$), which is approximately four times less than niobium and 25 times less than copper. The use of niobium as a substrate to platinum eliminates many of the problems with titanium; however, it is relatively costly. Copper, with its combination of high conductivity and low cost, is an ideal candidate for use as a current collector material.

In reviewing the properties of these materials, it becomes quite clear that if a combination of these materials could be developed that exploits only the advantages, the result would be a superior current collector material. The most logical combination of materials would include the use of a very thin platinum outer layer, for superior corrosion resistance and conductivity at limited cost; a niobium layer beneath the platinum to achieve dimensional stability; a copper expanded metal mesh core for both conductivity and economy [7].

The current collectors used in this study had a niobium expanded metal mesh core with a platinum coating. A copper metal mesh core with a platinum coating was not used because there are no commercial products available. A stainless steel expanded metal mesh with a gold coating was also used for comparison.

2.4. Hot-pressing MEA/GDL

An electrode-backing layer is placed on each side of the ion-conducting membrane, with a catalyst layer between each electrode-backing layer and ion-conducting membrane to form the five-layer MEA [15]. The electrode-backing layers and the ion-conducting membrane must be held closely together to reduce resistance to ionic and/or electrical flow between the elements. Ionic resistance exists in the catalyst layer and the electrolyte membrane. The elements can be held together by stack pressure, generally with two end plates ultimately applying the pressure. Ideally, the elements are laminated together – a process that also ensures physical proximity – as an alternative to using stack pressure. Lamination can be accomplished by using heat, pressure or a solvent. Heat lamination and solvent lamination also may involve the addition of some pressure. The appropriate methods for lamination depend on the materials.

In the heat lamination process, proton exchange membrane is sandwiched between the anode decal and cathode decal and is hot-pressed at 135 °C with 7.8×10^6 Pa for 5 min, thereby preparing the catalyst-coated electrolyte membrane (the Teflon substrate should be peeled off after cooling).

The cathode-backing layer and the anode-backing layer are bonded to the top surface of the catalyst-coated electrolyte membrane to form an MEA. Increasing adhesion at the edges of the MEA will greatly reduce the potential for delamination, because MEA delamination usually begins at the edges. It is preferable for the polymeric binder to be made of the same material as the membrane. Our case involved Nafion, which is com-

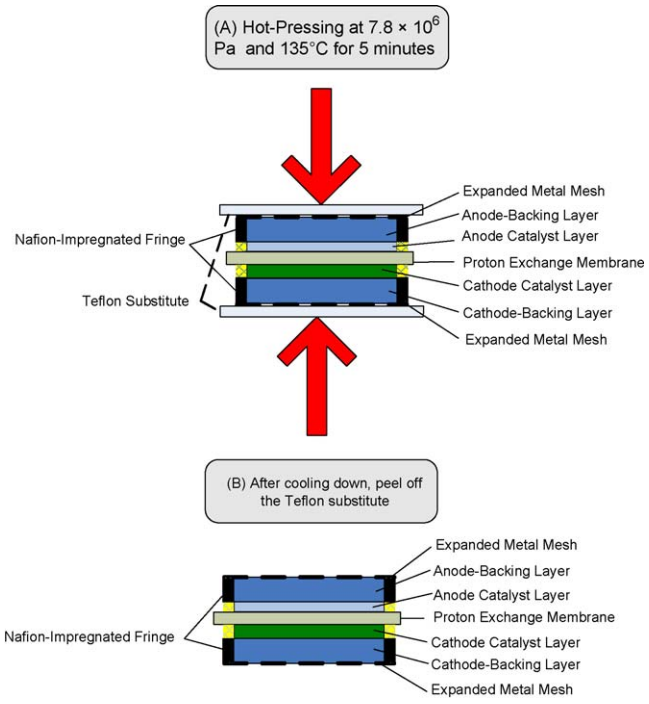

Fig. 4. The fabrication process of the membrane electrode assembly with enhanced bonding at edges. Step (A): the catalyst-coated membrane is sandwiched between the anode-backing layer and the cathode-backing layer and hot-pressed together. Step (B): after the MEA is cooled to the ambient temperature, the Teflon substitute is peeled off.

monly sprayed at the interface of the carbon-backing and catalyst layers. Nafion is not electrically conductive and increases the electrical resistance of a fuel cell. To solve this problem, a carbon-backing layer whose area is larger than that of the catalyst layer may be used. The fringe of the carbon-backing layer and the membrane will be bonded for the purpose of increasing bind. The fringe of the carbon layer can be integrated with the Nafion suspension (i.e., 10% Nafion in a water aliphatic alcohol mixture), as shown in Fig. 4. When the carbon-backing layers and the catalyst-coated membrane are hot-pressed together as shown in Fig. 4, a binding-enhanced fringe will be formed. After curing at 135 °C for 5 min, this fringe bonding becomes strong and can prevent delamination at the edges.

To bond metal mesh to the top surface of the carbon-backing layer, a similar procedure can be applied, as shown in Fig. 4. The edges of the metal mesh are dipped for 1 min in a solution of 10% Nafion suspended in a water aliphatic alcohol mixture and then air-dried. The U-shape metal mesh is hot-pressed with the carbon-backing layer and the catalyst-coated membrane to form a seven-layer MEA structure like that shown in Fig. 4B. This seven-layer MEA is ready for insertion into a window frame to form a planar fuel cell stack.

2.5. Assembly

To make a single cell, the above-mentioned seven-layer MEA, with a piece of thermo-bond film (pre-cut to the configuration of a gasket), is sandwiched between two fixture structures, and hot-pressed at 135 °C with a pressure of 70–140 kPa for 2–5 s. Thermo-Bond Film 615 (available from 3 M Electronics Adhesives and Specialties Department, Engineering Adhesives Division) serves as an adhesive bond and gasket. To make a bond using Thermo-Bond Film 615, the adhesive film can be first tacked (lightly bonded) to the window frames using low heat (40 °C, 1–2 s dwelling time, 35.0 kPa). The liner is then removed and the cells are placed between the two window frames. Heat and pressure are applied to form the bond.

To achieve a greater and more useful potential, multiple cells are connected in series. A planar fuel cell stack is shown in Fig. 5A. A common current collector was used to connect adjacent cells, as shown in Fig. 5B. This four-cell stack had a total active area of 18.0 cm^2 and stacks with an active area of 36.0 cm^2 were also made.

3. Results and discussion

The performance of the fuel cells created in this study was determined by a series of tests, which examined the cell's polarization curves, methanol concentration effects, self-heating effects and power density. The tests consisted of filling the anode active area with different methanol solutions then applying a load to the cell and measuring its corresponding voltage. The temperature of the cell and ambient conditions were also measured to determine the effects of temperature and humidity on cell performance. Single cells were tested first to determine which methods of making the cell were better and to obtain a base set of data. Stacks based on the single cell fabrication techniques were tested to find their polarization curves and long-term power outputs.

A Keithley 2440 5A Source Meter® was used to apply a load to the cell. Data collection was performed by a PC, which communicated with the load box through a GPIB card obtained from National Instruments, Inc. The cell voltage was also monitored using a METEX M-4650 voltmeter, and the cell temperature was measured using a FLUKE 32II thermometer. A thermocouple was fixed to the fuel cell's active surface area and an additional thermocouple was used to measure the room temperature. A humidity meter (obtained from Fisher Scientific, Model: 11-661-9) was used to measure the relative humidity of air.

3.1. Single cell performance

The first tests, on single cells, focused on current collectors and hot-pressing the MEA/GDL. Larger single cells were created to achieve a higher power output. The next series of tests showed the effects of methanol concentration on the cell's performance. The effect of temperature rise on cell performance was also examined.

3.1.1. Current collectors and hot-pressing MEA/GDL

To investigate the effects on single cell performance of current collectors and hot-pressed MEA/GDL, three single cells with an active area of 1.0 cm^2 were used with a frame structure found in Fig. 2A. The metal meshes had identical hole size and open area, 66%. Mesh no. 1 had a stainless steel core with a gold coating layer and a total thickness of 0.16 mm.

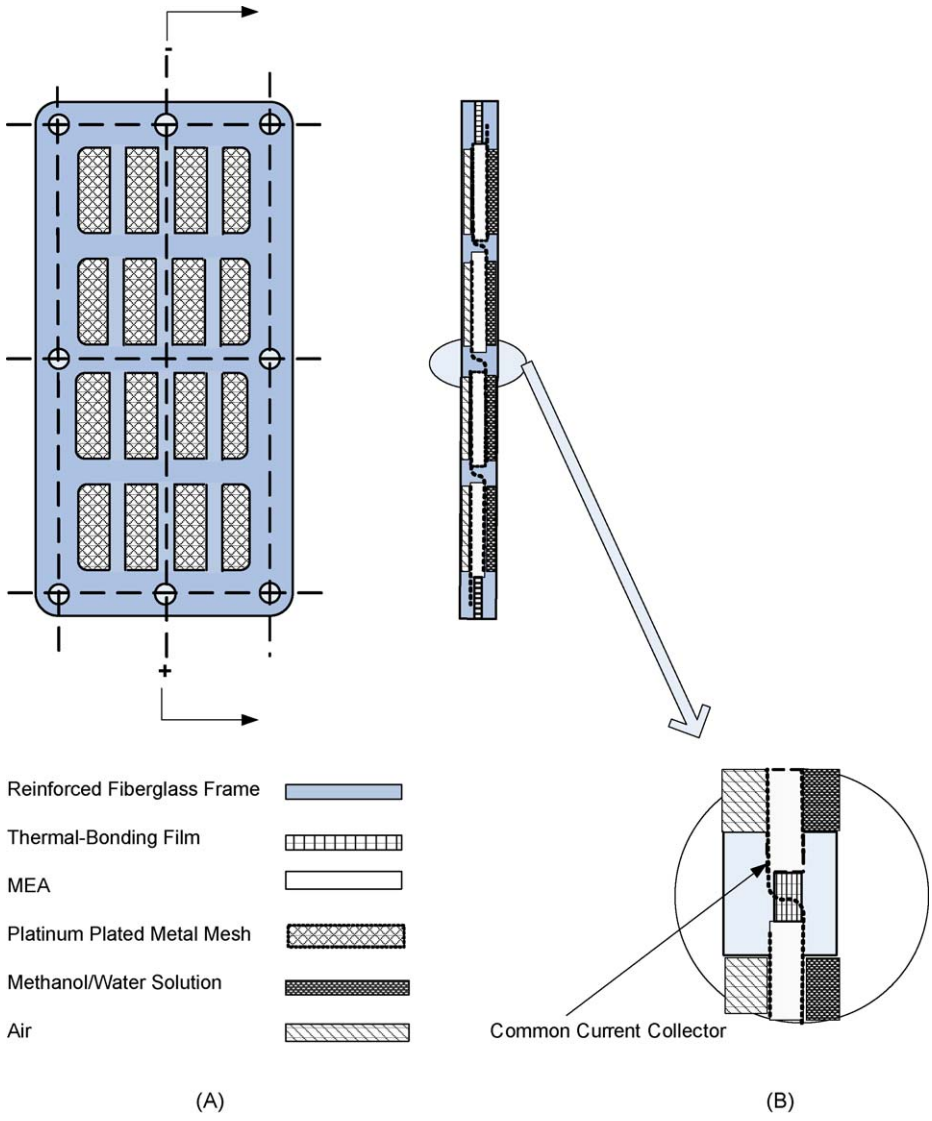

Fig. 5. A four-cell stack with the window-type fixture frame structure suitable for air breathing and fuel diffusion. (A) Four-cell stack; (B) an enlarged view of interconnections between adjacent cells by using a common current collector.

Mesh no. 2 had a niobium metal mesh core with a platinum coating layer and a total thickness of 0.54 mm. These two kinds of metal meshes were used due to their availability. The first cell used mesh no. 1 with a hot-pressed MEA/GDL, as described in Section 2.4, and the other two cells used mesh no. 2 for the current collector, only one of which had a hot-pressed MEA/GDL. The three cells were tested and results can be found in Fig. 6.

The cell that used mesh no. 1 demonstrated the poorest performance, achieving a maximum power density of only 11.8 mW cm^{-2}. The performance of the cells using mesh no. 2 was superior to that of the cell that used mesh no. 1. The cells with hot-pressed MEA and mesh no. 2 achieved the greatest power density. Based on these experiments, it can be concluded that the fabrication process that achieves the highest power density is the hot-pressed MEA/GDL procedure with mesh no. 2 as the current collector. This process was used on all subsequent fuel cells. To check these test results, another 1.0 cm^2 fuel cell was created with a hot-press MEA/GDL and mesh no. 2. The cell was tested in the same manner as before and produced very similar results, which can be seen in Fig. 7. The maximum power density achieved was 18.8 mW cm^{-2} at 75.0 mA cm^{-2} with a 2.0 M methanol solution.

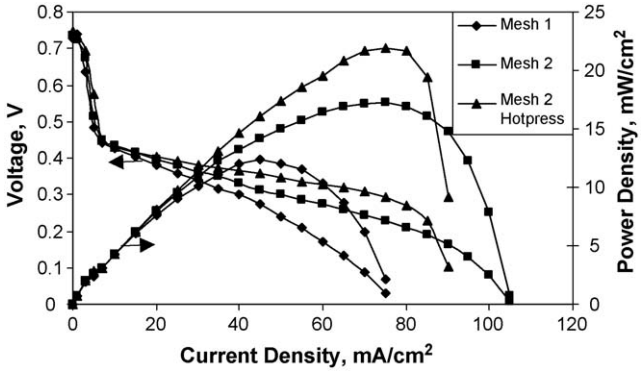

Fig. 6. Effects of current collectors and the hot-press MEA/GDL process on the single cell performance. A 2.0 M dilute methanol solution was used.

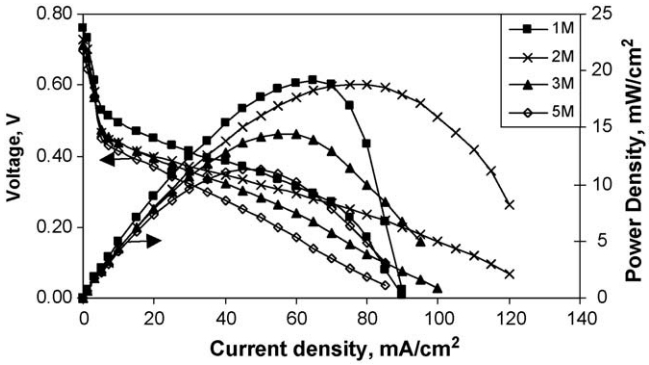

Fig. 7. The performance of a single cell with an active area of 1.0 cm^2.

3.1.2. Larger single cells

To achieve higher power output, cells with larger active areas are needed. A single cell was fabricated with a square active area of 6.25 cm^2, using a frame structure without ribs. The performance of this cell, as can be seen in Fig. 8, was poor when compared to the cell with an active area of 1.0 cm^2. It was determined that the contact resistance of the larger cell was too high and that structural support was needed in the middle of the cell. The next two cells incorporated ribs into the frame to minimize contact resistance by applying compressive force on the elements. They featured active areas of 4.5 and 9.0 cm^2, respectively, with ribbed frames as shown in Fig. 2B and C. This design produced a power density of more than 20 mW cm^{-2}, while the rib-less design achieved a power density of only 10.6 mW cm^{-2}.

These two new ribbed cells of 4.5 and 9.0 cm^2 produced very similar results during testing; each single cell achieved a power density between 20.0 and 25.0 mW cm^{-2} with the best results occurring when a 2.0 or 3.0 M methanol solution was used. The results appear in Fig. 9.

3.1.3. Methanol concentration effects

Four different methanol concentrations were examined: 1.0, 2.0, 3.0, and 5.0 M. For 1.0 M methanol solution the fuel cells operate well, but do not achieve high power densities. This is due to the low mass transport limitation of 1.0 M solution, which restricts the fuel cell from operation at high current densities (greater than 20.0 mA cm^{-2}). The fuel cell can operate

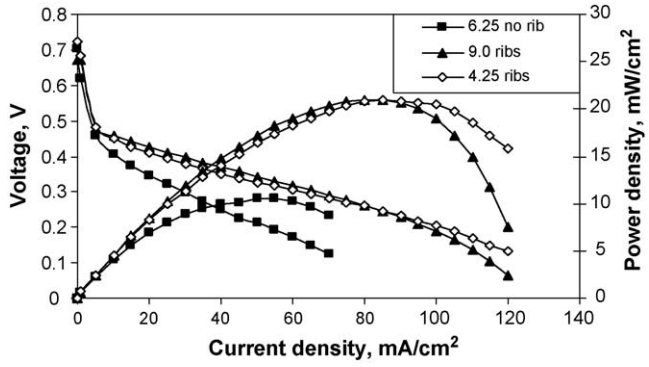

Fig. 8. Effects of the fixture frame structure on the single cell performance. A 3.0 M methanol solution was used.

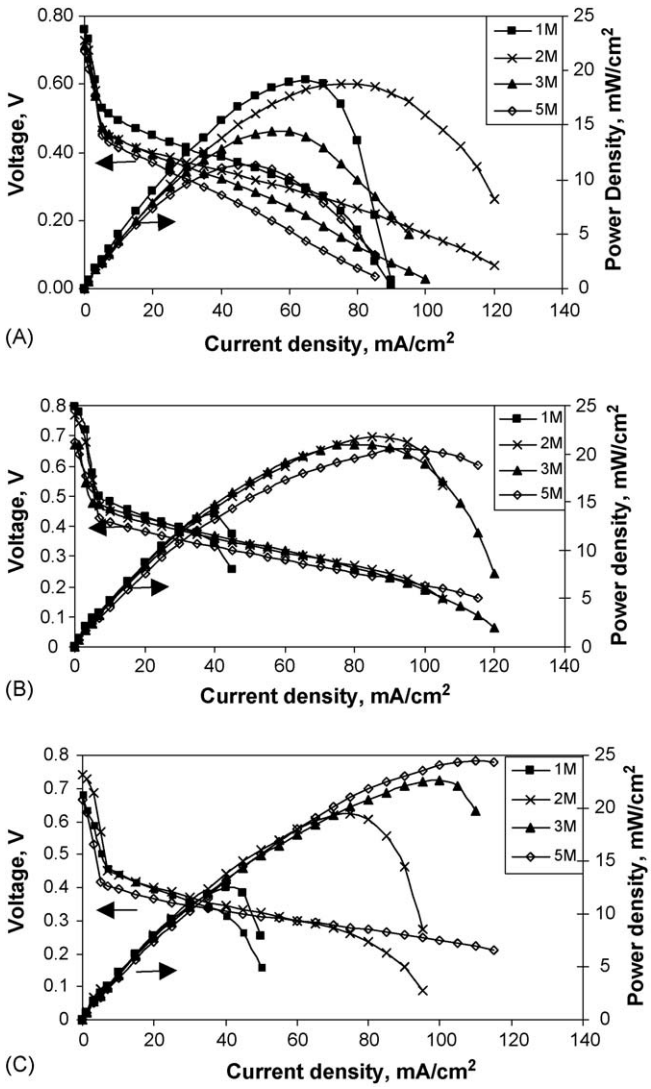

Fig. 9. The power density plots of single cells with different methanol concentrations. Active surface area (A) 1.0 cm^2 as shown in Fig. 2A; (B) 4.5 cm^2 as shown in Fig. 2B; (C) 9.0 cm^2 as shown in Fig. 2C.

only for short periods of time because the methanol in the solution is depleted quickly. The cell also does not experience a high temperature rise, due to the lower methanol crossover and lower electro-chemical reaction. If the cell is operated at current densities less than 20 mA cm^{-2}, 1.0 M solution is acceptable.

The cells' best performance occurs when 2.0 and 3.0 M methanol solutions are used. As shown in Fig. 9, the cell is capable of reaching over 20.0 mW cm^{-2} with these solutions. The cell experiences moderate temperature rises, as shown in Figs. 10 and 11, which increases the performance with less methanol crossover than in 5.0 M solutions. The mass transport limitation shifts to higher current densities as the concentration of methanol is increased in the solution. The overall performance for 2.0 and 3.0 M solutions is generally higher than 1.0 and 5.0 M solutions for current densities greater than 20 mA cm^{-2} as shown in Fig. 9. The maximum power density for 2.0 and

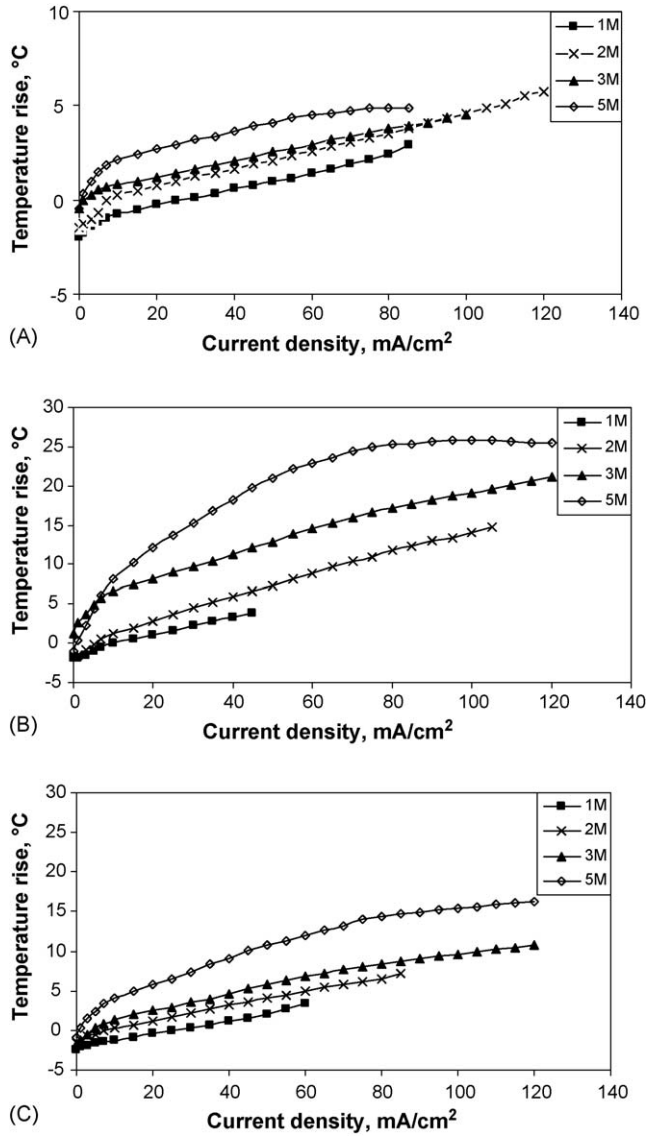

Fig. 10. The cell temperature rises vs. current density of the single cell DMFCs. Active surface area (A) 1.0 cm^2 as shown in Fig. 2A; (B) 4.5 cm^2 as shown in Fig. 2B; (C) 9.0 cm^2 as shown in Fig. 2C.

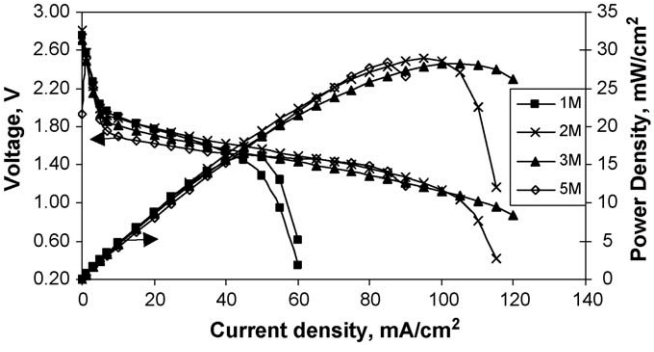

Fig. 11. The polarization and power output plots of the four-cell stack with total active area of 18 cm^2.

3.0 M solutions occurs at current densities between 80.0 and 100.0 mA cm^{-2}, which is significantly higher than current densities reached with 1.0 M solutions.

When a 5.0 M methanol solution is used, the performance decreases and the temperature rise of the cell increases dramatically. The higher methanol concentration permits greater methanol crossover, considerably increasing the temperature but reducing the power density. The 5.0 M solution reaches maximum performance of 20.0 mW cm^{-2} at a current density of 100.0 mA cm^{-2}, as shown in Fig. 9B and C.

The 2.0 and 3.0 M methanol solutions, in this study, are the best choice for dilute fuel for these passive air breathing DMFCs at ambient conditions (25 °C and 40–45% humidity). They produced the highest power density with modest methanol crossover and, thus, yielded the greatest efficiency. The 1.0 M solution is restricted in performance by methanol mass transport limitation and the 5.0 M solution has high methanol crossover, which is highly undesirable.

3.1.4. Self-Heating effects

A passive DMFC fuel cell works under mass diffusion conditions at both the anode and cathode sides. There is no forced-convection mass flow at the outer surface of the electrodes. The heat produced in the MEA area of the cell dissipates to the surroundings via evaporative cooling and natural convection. The MEA increases to a temperature higher than that of the surrounding air. The temperature of a passive single fuel cell increases with increased methanol concentration as a result of irreversible processes in the electro-chemical reaction and greater methanol crossover [8,16]. When a dilute methanol solution was used, the solution diffused to the cathode. Methanol in the solution reacted with air at the cathode to produced heat and water. Liquid water at the cathode (from diffusion and methanol catalytic reaction) evaporated, which cooled down the cell. The latter process dominated lower concentration methanol solutions, especially under the OCV condition, resulting in a cell temperature lower than the ambient temperature such as in the cases of 1.0 and 2.0 M. In Fig. 10A–C, it can be seen that 1.0 M solutions have a small temperature rise compared to 3.0 and 5.0 M. The 5.0 M solution has the greatest temperature rise, due to methanol crossover, and can increase 25 °C over room temperature, as seen in Fig. 10B. The temperature rise for 2.0 M is only a couple of degrees Celsius greater than 1.0 M but the performance increases dramatically, because of less methanol transfer limitation. The difference in temperature rise between 2.0 and 3.0 M is very small and has little effect on the performance of the cell in term of power density. The temperature rise for 5.0 M is much larger than for 3.0 M, but the power density decreases for 5.0 M, suggesting that more methanol is being consumed but not producing any additional power.

Maintaining an optimal temperature range is very important for cell performance. If the temperature is too low, the cell will not function properly. The cell needs to be at a high temperature to achieve a high power output. Since the cell performs better with a higher temperature, the self-heating is a positive effect for the cell as long it is not due to methanol crossover.

3.2. Stack performance

To create a more useful potential and greater power output the single cells are combined in a series to create a stack. The performance of these stacks and their extended testing results are discussed in the following section.

3.2.1. Four-Cell stack performance

The first stack design is based on the frame design shown in Fig. 2D. The stack has four cells of 4.5 cm^2, with a cumulative active area of 18.0 cm^2. The stack was tested with four different methanol solution concentrations: 1.0, 2.0, 3.0 and 5.0 M. The results from these tests are shown in Fig. 11. The ambient air temperature ranged from 23 to 25 °C with a relative humidity of 40–45%. When 1.0 M solution was used, the cell's voltage declined sharply at 50.0 mA cm^{-2}, which indicates inherent limits on methanol mass transport. The other solutions did not experience this sharp decline in voltage until about 120.0 mA cm^{-2}. The 2.0, 3.0 and 5.0 M solutions all achieved high power outputs of over 500.0 mW.

Another stack design is based on the fixture frame design shown in Fig. 2E. The planar stack with four cells has a total external area of 81.0 cm^2. Each cell has an active area of 9.0 cm^2 for a total active area of 36.0 cm^2. For structural integrity and to prevent cross talk, it is necessary to have a gap of a few millimeters between cells, but this reduces the active surface area to 44% of the total area. Fig. 12A shows the effect of the different methanol concentrations on the cell polarization curves. These curves were obtained by using methanol solutions of 1.0, 2.0, 3.0 and 5.0 M, respectively. For the 1.0 M methanol solution, the stack voltage decreases sharply when the current density approaches 60.0 mA cm^{-2}, which indicates significant limits on methanol mass transport. Additionally, the methanol concentration gradient through the anode GDL is not high enough to supply methanol to the anode catalyst layer. The polarization and power output plots of the four-cell stack have been investigated at a room temperature of 25 °C and a relative humidity of 45% (see Fig. 12). The 2.0 M solution produced the highest power density of 24.2 mW cm^{-2}, and all the solutions other than 1.0 M were stable at current densities up to 120.0 mA cm^{-2}.

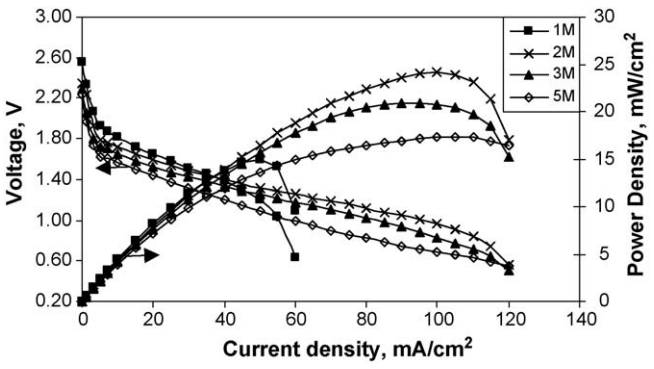

Fig. 12. The polarization and power output plots of the four-cell stack with total active area of 36 cm^2.

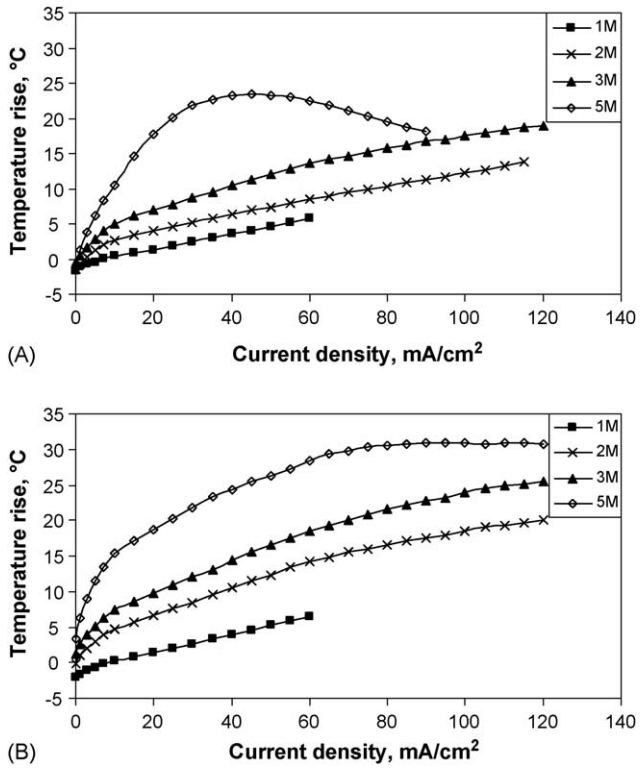

Fig. 13. The cell temperature rises vs. current density of the four-cell stacks. Active surface area (A) 18.0 cm^2 as shown in Fig. 2D; (B) 36.0 cm^2 as shown in Fig. 2E.

Since evaporative cooling is prevalent, the larger cell active area leads to larger diffusive length scales and slower evaporation. The fuel cell stacks experience a greater increase in temperature for a given methanol concentration than single cells, as can be seen in Fig. 13. Fig. 13B shows a larger temperature rise than Fig. 13A because the cell has twice the active surface area. The stacks tend to perform better than the single cells, most likely due to their higher operating temperatures.

3.2.2. Extended performance

To determine the fuel cell stack's performance over an extended period of time, the fuel cell stack with an active area of 18.0 cm^2 had a reservoir attached to the anode side of the fuel cell. This reservoir was then filled with a predetermined amount of solution. The test involved measurements, every 2 min, of the stack's current, the stack's temperature, and the ambient temperature.

To test the effects of methanol concentration on extended performance, 5.0 g of 2.0, 3.0 and 5.0 M methanol solutions were used in different tests. The tests were conducted at a constant voltage of 1.2 V under the ambient temperature of 25 °C and the relative humidity of 75%. The results of the tests are shown in Fig. 14A. The 2.0 M solution had an operating power density of about 16.0 mW cm^{-2} and stayed consistent for 40 min, after which point the power density decreased as the methanol concentration was depleted. The 3.0 M solution had an operating power density of about 12.0 mW cm^{-2} and held this power output for 80 min before the solution was

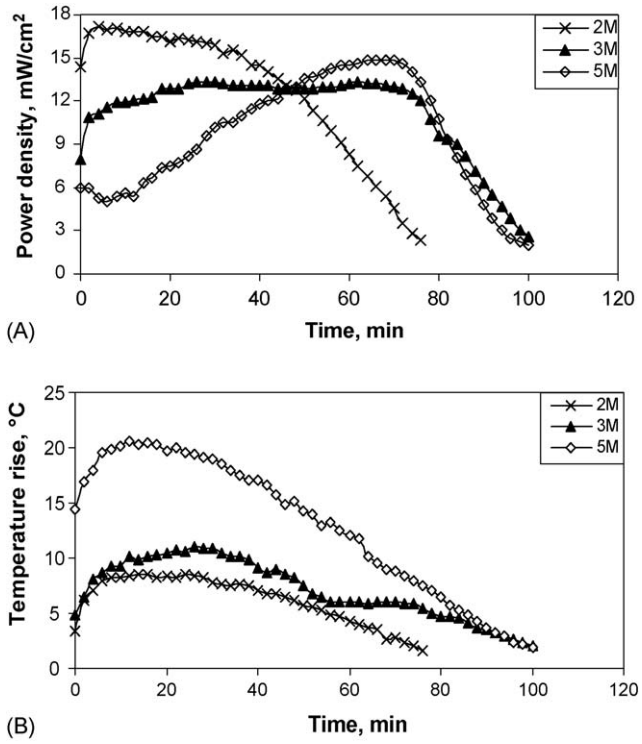

Fig. 14. Plot of constant stack potential test vs. different methanol concentration on a four-cell stack with an active area of 18.0 cm^2 at ambient conditions. (A) Power density and (B) temperature rise above the ambient temperature over the course of the test.

depleted. For 5.0 M methanol solution, the initial power density was only 6.0 mW cm^{-2}. The power density increased slowly to about 14.0 mW cm^{-2} in 60 min. This long power density-rise time might have been caused by the increase in methanol crossover that was experienced due to the higher concentration of methanol, as explained in Section 3.1.3. Fig. 14B shows that the temperature rise for 5.0 M solution was very high when compared to 2.0 and 3.0 M—about double the temperature rise. The temperature increment was around 15 °C with 5.0 M methanol operation at the beginning. Even through there was no electrochemical reaction at this moment, methanol diffused to the cathode and reacted with air at the cathode which heated the cell to a higher temperature. The higher methanol concentration permits greater methanol crossover such as 5.0 M solution in this case, considerably increasing the cell temperature. The higher temperature rise corresponded to more heat released to the ambient air. This shows that most of the energy content in the 5.0 M solution was being converted into heat and not electricity at the beginning of the test. After 60 min the 5.0 M solution had depleted enough so that the methanol crossover effect was reduced and more energy was being converted to electricity instead of heat. The power density became more consistent and resembled the behavior of 2.0 and 3.0 M solutions. After 80 min the power density decreased due to depletion of methanol in the solution. To calculate the methanol solution consumption of each solution, the remaining fluid in the fuel tank was weighed and subtracted from the initial weight. The fuel cell consumed 2.14, 2.47 and 4.06 g of 2.0, 3.0 and 5.0 M methanol solution, respectively.

The total electrical energy generated for each solution can be calculated by integrating the areas under the curves in Fig. 14A. The stacks produced total electrical energies of 1043.6, 1223.4 and 1044.6 J from 2.0, 3.0 and 5.0 M methanol solution, respectively. Assuming methanol was depleted in the 5.0 g solution, the overall efficiency is 15.0, 11.8 and 6.0% for the 2.0, 3.0 and 5.0 M solutions, respectively. Another measure of the fuel cell efficiency is known as the voltage efficiency and is the ratio of the actual voltage under operating conditions to the theoretical cell voltage. For the four-cell stack running at a constant voltage of 1.2 V, the single cell operating voltage is 0.3 V. The theoretical voltage of a DMFC is 1.2 V. The voltage efficiency is about 25%.

The fuel utilization efficiency is the ratio of the fuel that actually reacts in electrochemical reaction to the fuel input to the cell [1]. It can be simply calculated as the ratio of overall efficiency to the voltage efficiency, which is 0.15/0.25 = 60.0% for 2.0 M methanol solution, and is 47.2 and 24.0% for 3.0 and 5.0 M methanol solution, respectively. Fuel utilization efficiency losses may arise through methanol crossover and vaporization into the ambient air.

To test the effect of voltage on cell performance over time, a 2.0 M solution was tested under constant voltages of 1.2 and 1.4 V. The 1.2 V test had a higher power density than that of the 1.4 V test: 17.1–10.6 mW cm^{-2}, as shown in Fig. 15A. However, the 1.2 V test was not as steady as the 1.4 V test, due to the higher load. The 1.4 V test was more consistent over the 80 min test period because the solution was not exhausted as quickly, which explains why the 1.2 V test declined more sharply in power density after 40 min. The temperature rise of the two

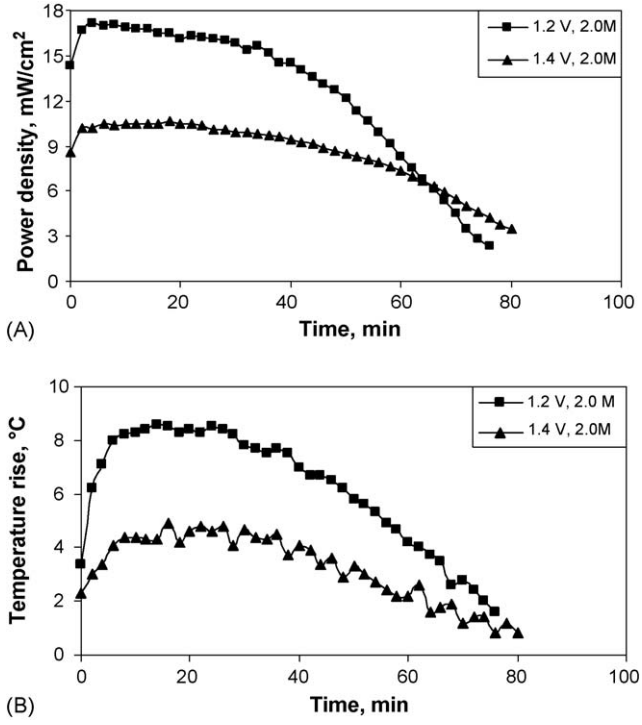

Fig. 15. Plot of constant stack potential tests at two different stack potential values on a four-cell stack with an active area of 18 cm^2. (A) Power density and (B) temperature rise above the ambient temperature over the course of the test.

tests is shown in Fig. 15B. The 1.2 V test has a higher temperature rise than the 1.4 V test because of its higher load. The stack produced total electrical energy of 1043.6 and 739.1 J at an overall efficiency of 15.0 and 10.6% for the 1.2 and 1.4 V tests, respectively. This is a surprising result. Fuel cells operated at higher voltage have higher voltage efficiency. The overall efficiency of the 1.2 V test is higher than 1.4 V testing in the case. It is surmised this outcome results from higher fuel utilization efficiency in the 1.2 V test. The corresponding operational current density for the power density curves in Fig. 15A is about 50.0 and 30.0 mA cm^{-2} for the 1.2 and 1.4 V tests, respectively. The higher operational current densities are usually associated with lower methanol crossover, producing higher fuel utilization efficiency in this particular testing case.

4. Conclusions

The planar fuel cell stack structure facilitates the diffusion of fluids (reactants and byproducts) into and out of the cell and is suitable for portable power source applications. A discussion of planar air breathing direct methanol fuel cell stacks has been presented with a detailed description of design and development procedures that began with small single cells, proceeded to large single cells, and then finally focused on stacks. Technical difficulties associated with each developing stage were overcome before moving to the next stage. A stack design is presented that is available in modules that can be configured to meet the power requirements of specific applications. The module design nature of the stack also makes it possible to fabricate the stack separately from other components of the fuel cell system. The selection criteria for GDL and current collectors were provided. The MEA and GDLs are laminated together to reduce electrical/ionic contact resistance, and this also helps to eliminate the associated heavy hardware. Methanol concentration has significant effects on output power density and cell operation temperature. The power density reached its highest value in this study when 2.0 and 3.0 M methanol solutions were used. The testing results of the four-cell stack showed that the highest power density of about 30.0 mW cm^{-2} was achieved at ambient conditions.

Acknowledgments

Authors would like to thank Dr. A. Smirnova for her kind help with making the catalyst-coated membranes, Dr. X. Huang for his assistance in setting up some of testing equipment and G. Jewett for his contributions to this study. All are associated with the Connecticut Global Fuel Cell Center, Storrs, CT, USA. Also, financial support from U.S. Army (Contract No. DAAB07-03-3-K-415) and National Science Foundation (Contract No. CTS-0514840) is gratefully acknowledged.

References

[1] M. Broussely, G. Archdale, Li-ion batteries and portable power source prospects for the next 5–10 years, J. Power Sources 136 (2004) 386–394.
[2] X.M. Ren, P. Zelenay, S. Thomas, J. Davey, S. Gottesfeld, Recent advances in direct methanol fuel cells at Los Alamos National Laboratory, J. Power Sources 86 (2000) 111–116.
[3] S.C. Thomas, X.M. Ren, S. Gottesfeld, P. Zelenay, Direct methanol fuel cells: progress in cell performance and cathode research, Electrochim. Acta 47 (2002) 3741–3748.
[4] A.S. Patil, T.G. Dubois, N. Sifer, E. Bostic, K. Gardner, M. Quah, C. Bolton, Portable fuel cell systems for America's army: technology transition to the field, J. Power Sources 136 (2004) 220–225.
[5] J. Larminie, A. Dicks, Fuel Cell Systems Explained, John Wiley and Sons, Ltd., 2002.
[6] C. Xie, J. Bostaph, J. Pavio, Development of a 2 W direct methanol fuel cell power source, J. Power Sources 136 (2004) 55–65.
[7] A. Faghri, Z. Guo, Planar fuel cell stack and method of fabrication of the same, US Patent Pending (2005).
[8] D.J. Kim, E.A. Cho, S.A. Hong, I.H. Oh, H.Y. Ha, Resent progress in passive direct methanol fuels in KIST, J. Power Sources 130 (2004) 172.
[9] J.G. Liu, T.S. Zhao, R. Chen, C.W. Wong, The effect of methanol concentration on the performance of a passive DMFC, Electrochem. Commun. 7 (2005) 288–294.
[10] X.M. Ren, Air breathing direct methanol fuel cell, US Patent No. 6,596,422 (2003).
[11] K. Choi, Monopolar cell pack of direct methanol fuel cell, US Patent No. 6,689,502 (2004).
[12] A. Faghri, Z. Guo, Challenges and opportunities of thermal management issues related to fuel cell technology and modeling, Int. J. Heat Mass Transfer 48 (2005) 3891–3920.
[13] J.A. Bett, D.J. Wheeler, C. Bushnell, Porous carbon body with increased wettability by water, US Patent No. 5,840,414 (1998).
[14] J.W. Frisk, W.M. Boand, Hydrophilic treatment of a carbon fiber construction, US Patent No. 6,733,841 (2004).
[15] C.Y. Chen, P. Yang, Y.S. Lee, K.F. Lin, Fabrication of electrocatalyst layers for direct methanol fuel cells, J. Power Sources 141 (2005) 24–29.
[16] B.K. Kho, B. Bae, M.A. Scibioh, J. Lee, H.Y. Ha, On the consequences of methanol crossover in passive air-breathing direct methanol fuel cells, J. Power Sources 142 (2005) 50–55.